LUND UNIVERSITY

FACULTY OF SCIENCE

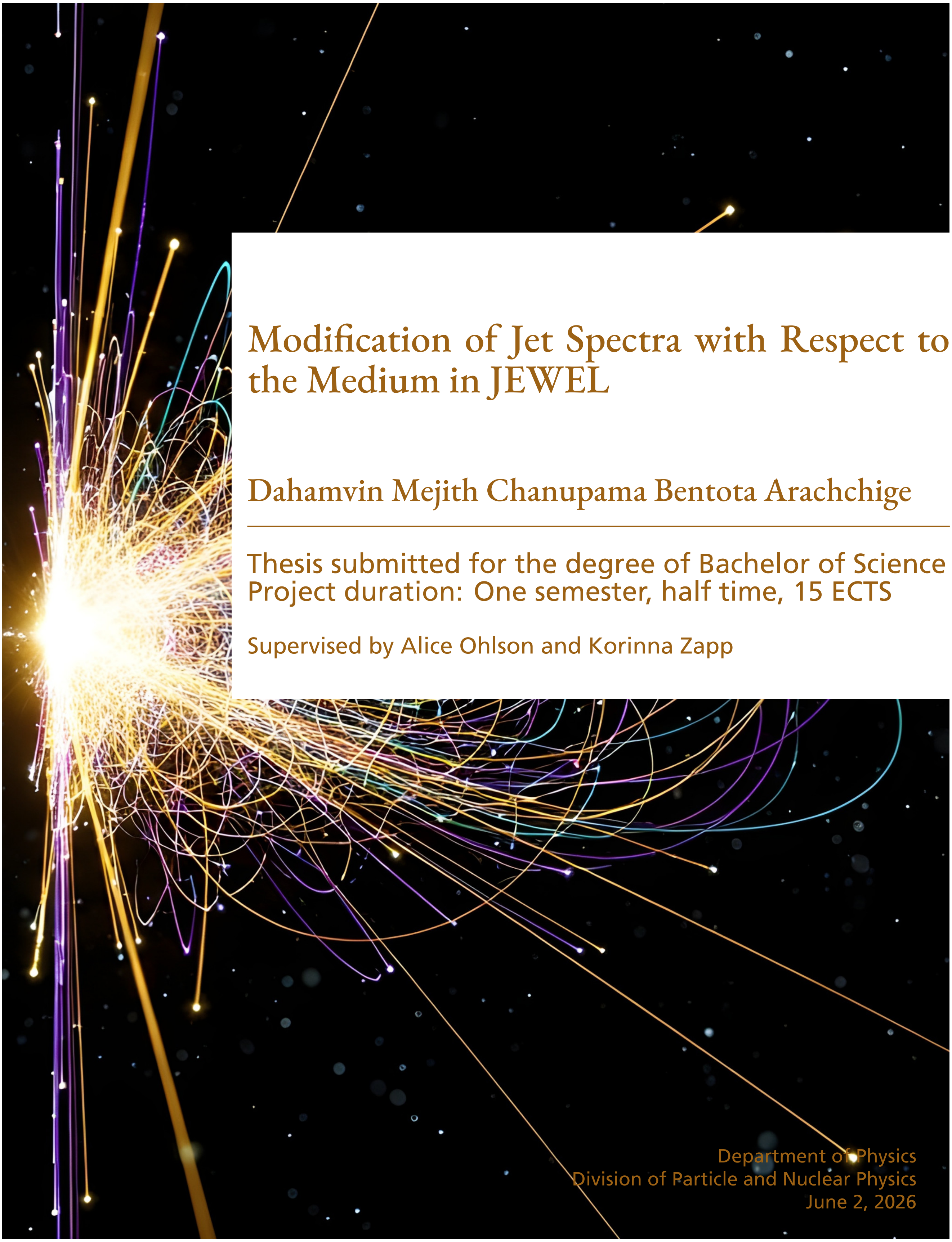

Modification of Jet Spectra with Respect to the Medium in JEWEL

Dahamvin Mejith Chanupama Bentota Arachchige

Thesis submitted for the degree of Bachelor of Science
Project duration: One semester, half time, 15 ECTS

Supervised by Alice Ohlson and Korinna Zapp

Department of Physics
Division of Particle and Nuclear Physics
June 2, 2026

Abstract

The goal of this thesis was to investigate the path-length dependence of jet suppression for jets propagating through a medium known as the quark–gluon plasma (QGP). The QGP is formed in collisions between two lead (Pb) ions, where the overlap region consists of participant nucleons distributed in an approximately elliptical geometry. Simulations of jet quenching in these collisions were performed using JEWEL together with the Glauber and Trajectum models. The former was used to describe the initial state, while the latter described the final state. Events containing jets were categorized according to their initial-state eccentricity ϵ_2 and their final-state elliptic flow, quantified by the parameter q_2. The jets were then further separated into in-plane and out-of-plane groups with respect to the short axis of the elliptical collision region. Across both models, out-of-plane jets were observed to be more suppressed than in-plane jets. This thesis successfully reproduced a measurement previously performed by the ALICE Collaboration at CERN. Furthermore, the results suggest that the observed path-length dependence is independent of the choice of models used, further validating its existence.

Keywords: Jet suppression, QGP, Path-length dependence

Acknowledgements

I would first like to thank my supervisor, Alice Ohlson, for her truly wonderful support, encouragement, and advice throughout the process of this thesis. I would also like to extend my gratitude to my co-supervisor, Korinna Zapp, for her expertise on JEWEL and her patience in handling all the errors we encountered in the first few weeks.

I am deeply grateful to my parents, Chamila Kumari Ratnayake and Lalith Kumar, for always being in my corner from the very beginning, for giving me the strength to keep going when things got tough, and, frankly, for making me the person I am today. I would also like to thank my aunt, Anoma Kumari Ratnayake, for her support and firm determination to bring me to Sweden so that I could pursue my bachelor's degree. I am equally grateful to Kevin Fernando, along with his parents, Mervyn and Sunethra Fernando, for their companionship and truly amazing food that never failed to bring me back home to Sri Lanka.

Additionally, I would like to express my gratitude to all the teachers and friends I have encountered throughout my life, both within and outside of school. I am extremely grateful to Niklas Simandi for his dedication to the formatting of this thesis, including the thesis template, as well as the polished diagrams produced from his code, and for his extraordinary advice and support as a true friend. I would also like to thank his parents, Conny and Claus Simandi, for welcoming me into their cosy home in Germany, taking great care of me while I was there, and allowing me to fully focus on my thesis during those two amazing weeks. I am also grateful to Ylva-Sophie Hohmeister for her valuable artistic input on the diagrams used in this thesis and for always helping me relax through pleasant conversation.

Furthermore, I would like to thank Sujin Maleesha Cooray and Gihan Sudeepa Bandara Pilapitiya for being my "unpaid therapists" every weekend and for always giving me valuable life advice. I am also grateful to Savinu Virunada Jayasuriya and Bineth Sarada Kumbukage for our conversations on physics, which have always kept me curious and entertained. I would also like to thank Shehara De Silva for her useful feedback and for being a constant companion in learning physics together despite living in two separate countries. Also, I would like to thank Lux Ruckstuhl, Gurjeet Kaur Chahal, Nikoleta Aikaterini Iakovatou, and Leeyla Bayar Mohammed for being wonderful friends, providing useful critique, and most importantly, lending an ear while I rambled about my thesis and physics in general. On that note, I would also like to thank my corridor neighbors, Hannah Zettel and Jennie Sandberg, for allowing me to entertain them with particle physics discussions. Finally, I would like to thank María Esther Vilar Alvarez for being the first friend I made at university and for recommending Alice Ohlson as my supervisor.

Contents

Chapter 1
Introduction and Background

1.1 Overview

When two heavy ions collide, the resulting energy causes the creation of a hot, dense medium called quark-gluon plasma (QGP) as well as particles with high momenta that spray in collimated beams called jets. Using data gained from Pb-Pb collisions, the ALICE collaboration released a study investigating path-length dependence for jets moving through the QGP [1]. Thereby, it becomes vital to simulate this phenomenon and attempt to investigate it. To this end, the goal of this paper is to use JEWEL, a Monte-Carlo event-generator, to analyze differences between jets traveling different path-lengths under varying factors that affect the geometry of the QGP, such as eccentricity.

This section begins with an introduction to Quantum Chromodynamics (QCD) and quarks, then moves on to jet formation. Afterwards, jet suppression is described, followed by an account of in-plane and out-of-plane jets and an overview of JEWEL. Next, the different models used in this thesis are presented. Chapter 2 details the parameters used in the analysis and the general strategy for evaluating the plots based on different factors such as eccentricity. A thorough analysis and discussion of these simulated results are provided in Chapter 3. Finally, Chapter 4 concludes with a summary of the project and provides an outlook on further investigations into path-length dependence in jet suppression.

1.2 Jet Production and Suppression

Quarks are considered to be point-like constituent particles that compose matter in the universe. They are governed by quantum chromodynamics (QCD) that give quarks two fundamental properties: asymptotic freedom and confinement. At high energy scales (short distances), quarks behave as if they are free and at low energy scales (long distances) they are confined. This is shown in Figure 1.1.

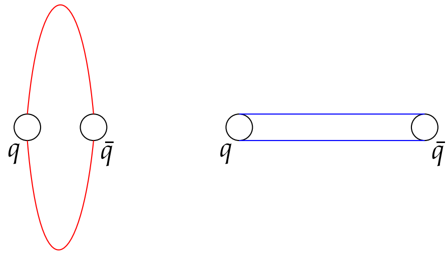

Figure 1.1: Asymptotic freedom (left) and confinement (right)

Using the analogy of a rubber band, when the quark and anti-quark (connected by gluons) are close to one another, the rubber is unstretched and loose, thereby the quark and anti-quark could move "freely" within those bounds.

But as shown on the right in Figure 1.1, when the band is stretched, they are constricted and therefore confined. At high energies in heavy-ion collisions, the quarks and gluons behave quasi-freely and become deconfined, thereby forming the QGP [6].

Early in the collision, hard scatterings produce high momentum quarks and gluons (collectively called partons). In a vacuum, these high energy partons would fragment into collimated sprays of hadrons, known as jets. But, in the case of the QGP acting as the medium, these energetic partons would interact with the medium and undergo elastic and inelastic scattering, and lose energy before fragmenting into hadrons [9]. This is known as jet quenching, and it can be used to investigate the QGP [6]. Furthermore, suppression is observed by obtaining the nuclear modification factor (R_{AA}), which is a ratio between jet measurements in proton-proton and heavy-ion (HI) collisions [11]:

$$R_{AA} = \frac{dN^{AA}/dp_T}{\langle N_{coll}\rangle\, dN^{pp}/dp_T}, \tag{1.2.1}$$

where dN^{AA}/dp_T, dN^{pp}/dp_T represents the number of jets as a function of their transverse momentum p_T, in Pb-Pb collisions, and proton-proton collisions respectively, and $\langle N_{coll}\rangle$ is the number of nucleon-nucleon collisions for a given centrality class [6]. We can note that suppression is observed when R_{AA} is less than 1, as there would be fewer jets in the Pb-Pb collision compared with an equivalent number of proton-proton collisions.

A centrality class is defined by the impact parameter $\boldsymbol{b}$ [8], which is a vector connecting the centers of the two colliding nuclei as shown in Figure 1.2. The geometry of the impact region when two Pb ions collide can be determined by the centrality and eccentricity of the collision. It can be seen that the smaller $\boldsymbol{b}$ is in magnitude, the more central the collision is and vice versa.

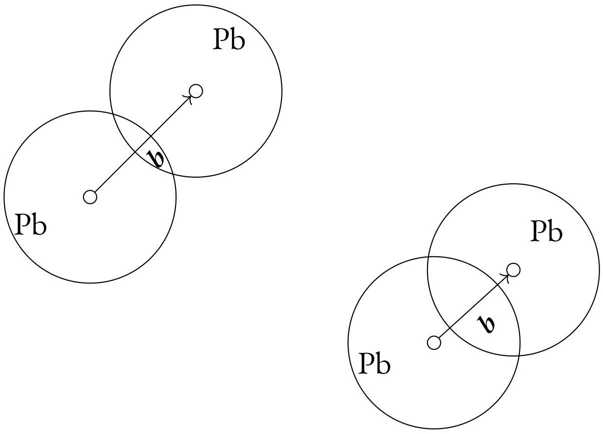

Figure 1.2: ***b*** in a more peripheral event (top left) and a more central event (bottom right), shown in the perspective of the plane transverse to the beam-line.

1.3 In-Plane and Out-of-Plane Jets

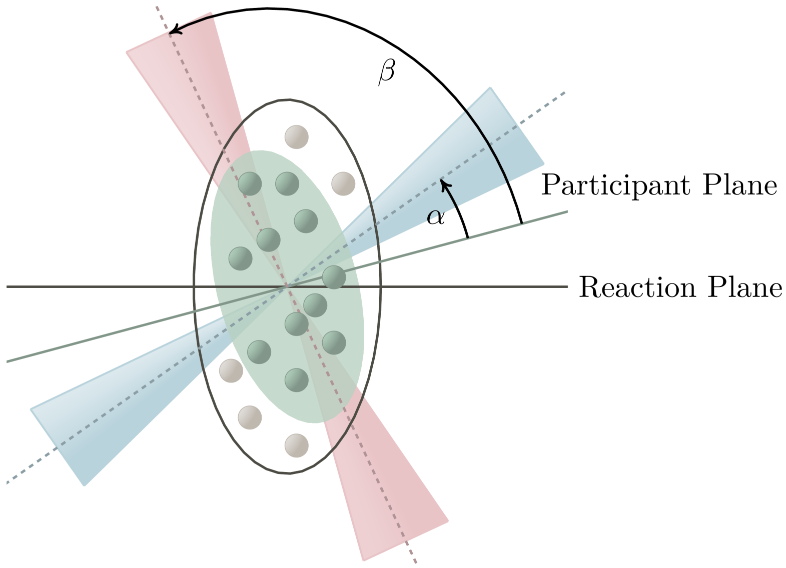

Figure 1.3: Sketch of in-plane (blue) and out-of-plane (red) jets. α represents an in-plane angle where $\alpha < \pi/6$ or $5\pi/6 < \alpha$ and β describes an out-of-plane angle where $\beta < 2\pi/3$ and $\beta > \pi/3$. Note that $0 \leq \alpha, \beta < \pi$. The nucleons inside the green ellipse are called participants, and those outside are called spectators.

As the colliding Pb nuclei produce an elliptical overlap region as shown in Figure 1.3, the QGP is anisotropic meaning that observations are dependent on the direction of measurement. Jets produced in the participant region include in-plane jets which are jets that mostly align with the participant plane or the event-plane (for the final state), thereby are near the minor axis of the green ellipse in Figure 1.3. As an example one could see that this is the case for the blue jets in Figure 1.3. Out-of-plane jets lie close to the major axis of the green ellipse and are almost perpendicular to the participant plane. Therefore, it is expected that out-of-plane jets would traverse a longer path-length in the medium, than in-plane jets, leading to more jet quenching, which would then depend on the angle of the jet axis with respect to the participant plane.

For the initial state, in-plane and out-of-plane jets can be defined from the angular difference $\phi_{\text{jet}} - \psi_{pp}$, where ϕ_{jet} is the azimuthal angle of the jet axis and ψ_{pp} is the angle of the participant plane. For the final state, the angular difference becomes $\phi_{\text{jet}} - \psi_{ep}$, where ψ_{ep} is the angle of the event plane.

This angular difference, for example for the initial state, can be rotated such that $-\pi < \phi_{\text{jet}} - \psi_{pp} < \pi$. Next, using symmetry, we can simply take the positive angular difference and reduce our angular range such that $0 \leq |\phi_{\text{jet}} - \psi_{pp}| < \pi$. Thereby, we can separate in-plane and out-of-plane jets such that if $|\phi_{\text{jet}} - \psi_{pp}| < \pi/6$ or $|\phi_{\text{jet}} - \psi_{pp}| > 5\pi/6$ we have in-plane jets. We can have out-of-plane jets if $|\phi_{\text{jet}} - \psi_{pp}| > \pi/3$ and $|\phi_{\text{jet}} - \psi_{pp}| < 2\pi/3$.

But conducting a jet spectra analysis only based on in- and out-of-plane definitions, produces a minor difference between the spectra. Therefore, highly elliptical events can be selected in order to use the anisotropy and demonstrate a difference in in- and out-of-plane jet spectra. For the initial state, eccentricity ϵ_2 is the variable used to define the ellipticity of the QGP, which is calculated using the polar coordinates of the participant nucleons, r and ϕ_{initial} as follows:

$$r = \sqrt{x^2 + y^2}, \tag{1.3.1}$$

$$\phi_{\text{initial}} = \arctan\left(\frac{y}{x}\right), \tag{1.3.2}$$

$$\epsilon_2 = \frac{\sqrt{\langle r^2 \cos(2\phi_{\text{initial}})\rangle^2 + \langle r^2 \sin(2\phi_{\text{initial}})\rangle^2}}{\langle r^2 \rangle}, \tag{1.3.3}$$

where $\langle \dots \rangle$ represents an average over the number of participant nucleons [2].

For the final state, the geometry of the QGP is described by a variable called q_2, known as the reduced flow vector [1]. This is found as follows:

$$q_2 = \frac{|Q_2|}{\sqrt{P_T}}, \tag{1.3.4}$$

where P_T is the sum of transverse momenta of final state particles, and Q_2 is the second harmonic flow vector which using the individual transverse momenta p_i and individual azimuthal angles ϕ_i is defined to be [1]:

$$Q_2 = \left(\sum_i p_i \cos 2\phi_i, \sum_i p_i \sin 2\phi_i\right). \tag{1.3.5}$$

We can use p_T in analysing jet suppression by looking at the number of jets produced that is plotted against their p_T for example as shown in the sketch Figure 1.4a. If a path-length dependency does exist, then it is expected that there would be fewer out-of-plane jets than in-plane jets but this difference is not always clear and evident. If the shape is largely elliptical with high q_2 then we would obtain Figure 1.4a, but if the shape were more circular (low q_2), we would obtain Figure 1.4b.

As the sketch in Figure 1.4b shows, the number of jets in-plane and out-of-plane are almost the same due to circular symmetry meaning that the jets traverse equidistant paths within the medium. But in the sketch Figure 1.4a, the in-plane jet moves across a shorter path than the out-of-plane jet, thereby leading to lower in-plane jet suppression. Therefore, by observing the extreme ends of the geometry, through event-shape engineering, we expect to observe a path-length dependency effect on jet suppression. The ALICE collaboration in CERN has conducted this analysis based on Run2 data,

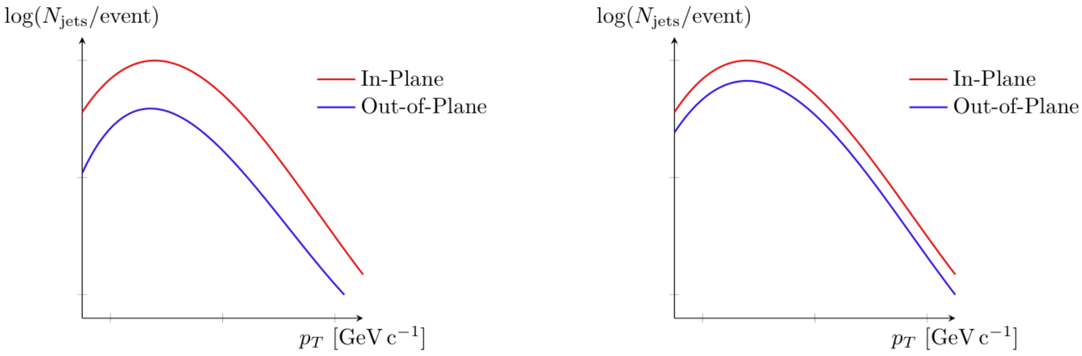

(a) Sketch of jet suppression with high q_2

(b) Sketch of jet suppression with low q_2

Figure 1.4: Comparison of in-plane and out-of-plane jets with (left) high and (right) low q_2. High q_2 events may show a larger difference in in-plane and out-of-plane suppression than low q_2 events.

and produced Figure 1.5 [1]. But no model comparison was performed, to show path-length dependence, which presents the main goal of this thesis.

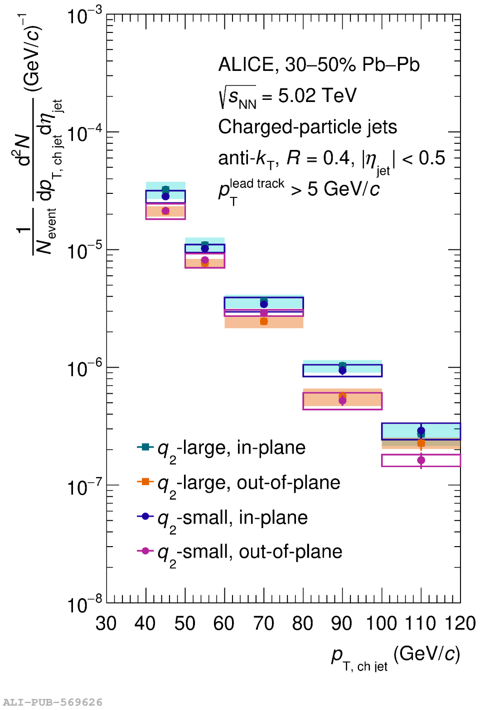

Figure 1.5: Charged particle jets for large and small q_2 classes for in-plane and out-of-plane jets found by the ALICE collaboration [1]

Now in order to conduct the model comparison, we first need to simulate heavy ion collisions using a Monte-Carlo (MC) event generator.

1.4 JEWEL

Jet Evolution With Energy Losses (JEWEL) is a MC event generator that simulates the evolution of a di-jet system using our understanding of particle interactions in heavy-ion collisions [16]. Furthermore, it describes the progression of jets in both a vacuum and a medium [15]. In order to model jet quenching in a medium, JEWEL views the medium as a collection of partons where we would observe scattering events that result in energy loss and basically modifies the intermediate parton shower where the interactions are believed to occur [16] [11].

There are two varieties of energy loss caused by a medium, collisional and radiative [3]. Collisional energy loss occurs when high energy partons interact with the medium but do not cause the emission of additional partons and radiative energy loss happens when these extra partonic emissions occur [16]. In a partonic shower, the hardness of the emitted partons are characterized by their transverse momentum, which decreases in the final state [3]. The initial state depends on the shape of the collision, and JEWEL firstly describes this initial geometry by using for instance the impact parameter b specified by the model used, and the jet creation point from the density of binary nucleon-nucleon collisions [16]. Then PYTHIA, a general purpose event generator, is incorporated in JEWEL, that provides the initial state parton shower which simulates the evolution of hard scattering processes [4][16].

Next, the final parton shower is generated by JEWEL which includes the two kinds of partonic energy loss discussed previously [16]. Afterwards, this event is sent back to PYTHIA to undergo hadronization, which is the process by which the final-state partons produced in hard scattering, form hadrons [16][14].

All these events are the result of jets interacting with the QGP, which we are interested in, and JEWEL enables us to conduct simulations that could be directly compared with experimental data. This makes it a great tool to study path-length dependence on jet suppression and analyse QGP, as it can be inserted into different models representing the initial and final states of the collision.

1.5 The Simple Model

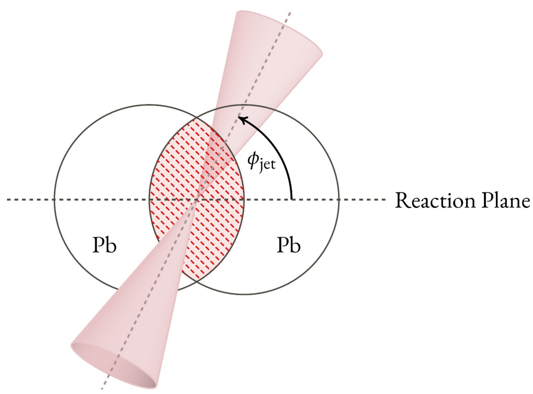

Figure 1.6: Simple model, where the collision region of two Pb nuclei is static, and ϕ_{jet} is the azimuthal angle of the jet axis with respect to the reaction plane.

The simple model provides a simplified perspective of the initial state by assuming that the region of collision is smooth, meaning that there are no fluctuations in the continuous nucleon distribution [3]. Furthermore the position of a jet creation point depends on the density of binary nucleon-nucleon collisions [3]. Additionally, to show the time evolution of the QGP, the energy density decreases in proportion to $\tau^{-4/3}$, where τ is the proper time [3]. JEWEL by default uses the simple model but since the eccentricity remains fixed, it is not useful for the goals of this thesis. Therefore, to simulate a more realistic model with shifting nucleons and varying eccentricities, the Glauber model should be used [3].

1.6 The Glauber Model

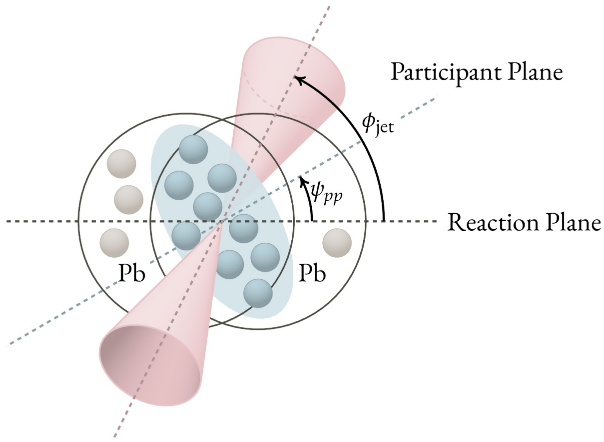

Figure 1.7: Glauber model where the collision of two Pb nuclei showcases randomized nucleon positions. The participant plane lies on the minor axis of the blue ellipse. ϕ_{jet} is the azimuthal angle between the jet and the reaction plane and ψ_{pp} is the angle of the participant plane with respect to the reaction plane.

The Monte-Carlo Glauber model begins by randomly generating the central positions of the nucleons in each nucleus, and afterwards randomly choosing the impact parameter b [3]. The sketch in Figure 1.7 shows nucleons within the blue elliptical region, which are called participants and those outside are spectators. Participants are defined to be a pair of nucleons from each of the two Pb nuclei, such that, during the collision, the distance between their centers is less than or equal to the diameter of an individual nucleon [3]. The positions of these nucleon-nucleon interactions also provide jet creation points as well [3]. Furthermore, the participating nucleon density is generated by plotting a two-dimensional Gaussian distribution that changes from event to event. This produces a more realistic shape for the QGP than the one described by the simple model. Additionally, from the nucleon-nucleon interactions, different observables can be computed, such as the participant plane angle ψ_{pp}, which is defined by first obtaining the x and y coordinates. Afterwards, for each participant, the azimuthal angle ϕ_{initial} can be found, and ψ_{pp} can then be calculated as follows:

$$\psi_{pp} = \frac{1}{2} \arctan\left(\frac{\langle \sin 2\phi_{\text{initial}} \rangle}{\langle \cos 2\phi_{\text{initial}} \rangle}\right) + \frac{\pi}{2}, \tag{1.6.1}$$

where $\langle \dots \rangle$ represents an average over the number of participant nucleons. Using the Glauber model changes the smooth continuous collision region (given in the previous simple case) to one with crests and troughs, that better simulates experiments. But using this model alone would not give us a complete picture of the final state because the QGP evolves as a fluid. Thereby, in order to properly encapsulate the medium environment, a model that includes hydrodynamic expansion is needed.

1.7 The Trajectum Model

As the QGP behaves as a fluid, it can be described by relativistic hydrodynamics which is valid when the mean free path of the partons is much smaller than the system itself [3]. Furthermore, this is permitted until just before the beginning of the hadronization stage [3]. Trajectum represents a model that computes initial conditions, a prehydrodynamic phase, a hydrodynamic phase and particlization [12].

The aforementioned Glauber model will be used as a basis for the initial state for Trajectum. Thereby, the preliminary geometry can be obtained from these initial conditions and pressure gradients that influence hydrodynamic expansion can be found [12]. Then during the prehydrodynamic phase, the partons in the QGP flow without scattering for a certain time period. Next, the QGP expands in the hydrodynamic phase leading to particles being boosted due to flow velocity [10], and Trajectum solves the relevant equations of motion during this period. Following the hydrodynamic phase, particlization occurs which is a process where the fluid is converted to final particle distributions [10]. Finally, the hadrons are then sent to hadronic transport codes such as SMASH that will look at consequent scatterings and decays [10].

Additionally, Trajectum provides the initial state eccentricity ϵ_2 which can be used to compare results with the Glauber model. Experimentally however, ϵ_2 can not be measured, since we can only observe the final state particles, and thereby the shape of the QGP is determined by q_2. For the final state, it is necessary to approximate the plane of symmetry, which is called the event plane. The event-plane angle ψ_{ep} is found using the final state particles' momenta, p_x and p_y in the x and y directions respectively:

$$\phi_{\text{final}} = \arctan\left(\frac{p_y}{p_x}\right), \tag{1.7.1}$$

$$\psi_{ep} = \frac{1}{2}\arctan\left(\frac{\langle \sin 2\phi_{\text{final}}\rangle}{\langle \cos 2\phi_{\text{final}}\rangle}\right), \tag{1.7.2}$$

where $\langle \dots \rangle$ represents an average over the number of final-state particles. Trajectum is highly useful in simulating experiments since it is a model that fully describes the evolution of the heavy-ion collision.

From these models, one can use the azimuthal jet angles ϕ_{jet} (provided by JEWEL), participant plane angles ψ_{pp} and event-plane angles ψ_{ep} to define in-plane and out-of-plane jets. Using these definitions, for high eccentric or q_2 events, one can look for a notable difference in the degree of in- and out-of-plane jet suppression which is observed in experiments as given in Figure 1.5. Performing this analysis provides greater insight into path-length dependence in jet quenching.

Chapter 2
Approach and Methodology

This section aims to provide a detailed description of the strategy used to reach the goal of the project. Firstly, a description of the main simulation parameters used will be given. Secondly, for each of the models, it is important to know what the bounds of certain parameters are. Such as, what are the limits of high q_2 or low eccentricity? These can then be used to separate events according to different use-cases. Finally, a discussion on connecting all the sections mentioned in this chapter will be conducted.

2.1 Glauber

Using JEWEL and the Glauber model, 1×10^6 Pb-Pb collision events were generated at a center-of-mass energy of $\sqrt{s_{NN}} = 5{,}02\,\text{TeV}$ and a centrality class of 30–50% was considered to simulate the experimental procedure conducted by the ALICE collaboration [1]. These events were stored in High Energy Physics Monte Carlo (HepMC) files, which include particle-level information as summarized in Table B.2 [7] and then were analysed using Rivet [5]. After plotting the eccentricity distribution as shown in Figure 2.1, a Python program was used to calculate the bottom 20% and top 20% of events, corresponding to low eccentricity and high eccentricity cuts, respectively.

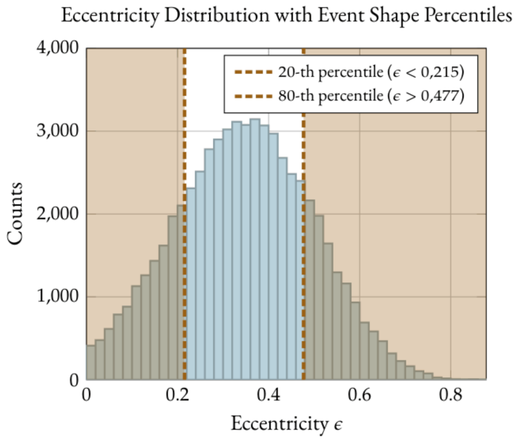

Figure 2.1: Eccentricity bounds found from taking the top 20 and bottom 20 percentiles for the Glauber model. High-eccentricity events have an eccentricity above 0.477 and low-eccentricity events, an eccentricity below 0.215.

2.2 Trajectum

To model the final state, Trajectum was used to generate 4000 collision profiles containing information about final-state particles. These profiles were filtered by using multiplicity percentiles of 70% and 50% to represent the 30 – 50% centrality class. The profiles were then filtered further to only include final-state charged particles, with a p_T cut of 0,2 GeV/c and a pseudo-rapidity cut $|\eta| < 1$. After this filtration process, the remaining 762 profiles were reused multiple times with JEWEL, and 8×10^5 collision events were produced, which were afterwards subjected to eccentricity and q_2 cuts as given by Figures 2.2 and 2.3. The eccentricity cuts were performed similarly to the Glauber model, with Python code used to identify the bottom 20% and top 20% of the eccentricity distribution shown in Figure 2.2, representing low- and high-eccentricity events, respectively.

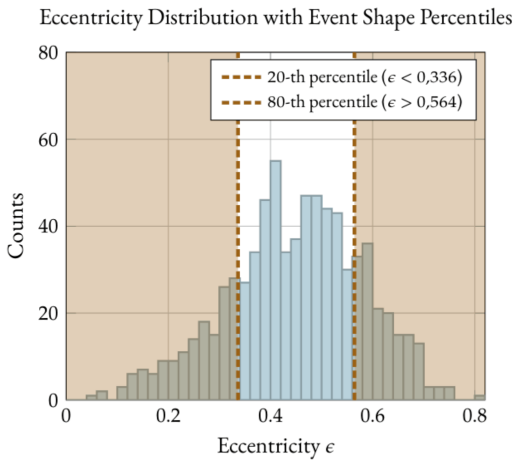

Figure 2.2: Eccentricity bounds found from taking the top 20 and bottom 20 percentiles for Trajectum. Low eccentric events would have an eccentricity lesser than 0.336 and high eccentric events would possess an eccentricity greater than 0.564.

After plotting the q_2 distribution, the q_2 cuts were defined as shown in Figure 2.3, using a Python program to determine the bottom 20% and top 20% of events, corresponding to low q_2 and high q_2 events, respectively.

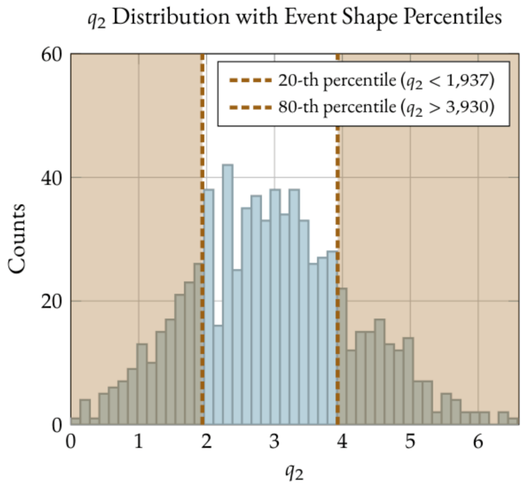

Figure 2.3: q_2 bounds found from taking the top 20 and bottom 20 percentiles. High q_2 events have a q_2 value greater than 3.930 and low q_2 events indicate a value lower than 1.937.

2.3 Analysis Summary

To summarize, initially JEWEL along with the Glauber model was used to produce events, which were then separated based on their eccentricities as given in Figure 2.1. Along with these eccentricity bounds, in-plane and out-of-plane jets were isolated as described in Section 1.3. Thereby, a plot comparing high eccentric and low eccentric events for both in-plane and out-of-plane jets was made. Next, a plot of in-plane versus out-of-plane jets was made, that was inclusive of both high and low eccentricities. Afterwards, path-length dependence was tested by producing plots of in-plane and out-of-plane jets under low and high eccentricities. The same was done for Trajectum, but with the eccentricity bounds given in Figure 2.2.

Furthermore, we can note that if similar results are found for Trajectum as Glauber, based on eccentricity, then it further validates path-length dependence in jet suppression. Next, a plot of the jet spectra in high q_2 versus low q_2 events was made using Trajectum with the bounds described in Figure 2.3, that was inclusive of both in-plane and out-of-plane jets. Following this, in-plane and out-of-plane jets were plotted against each other, including both high and low q_2 events. Finally, in-plane and out-of-plane jets were plotted under low and high q_2 ranges. These were used to show path-length dependence in jet suppression for the final state.

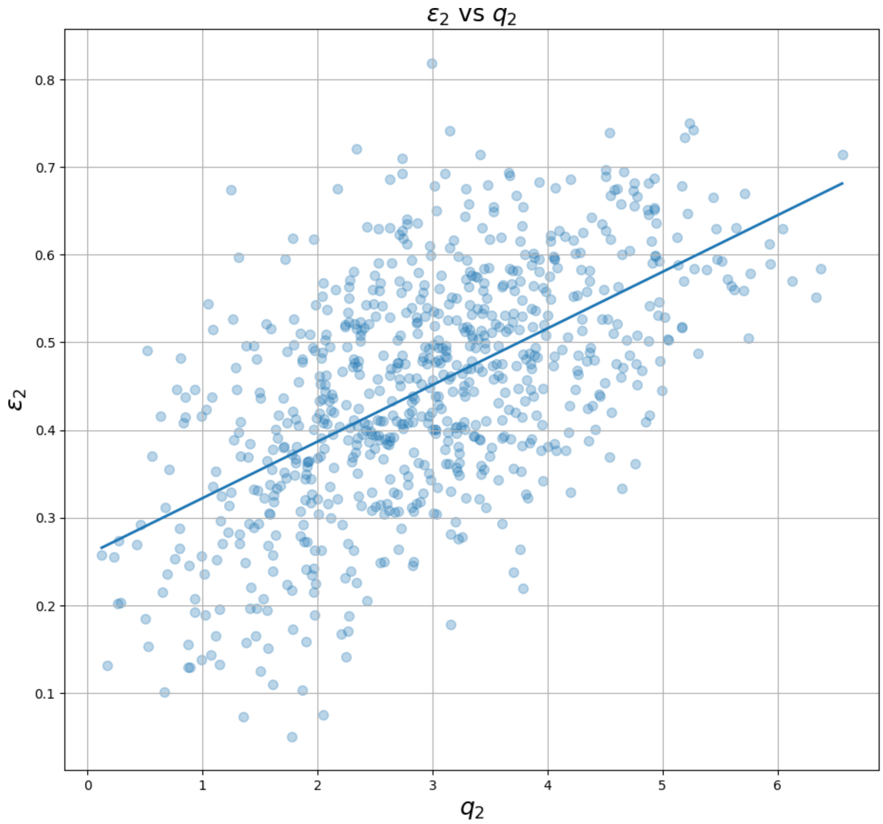

Figure 2.4: Plot of eccentricity (ϵ_2) vs q_2 showing a linear correlation.

Additionally, it is to be expected that q_2 events, whether high or low in magnitude, are similar to eccentric events of the same magnitudes, because, as shown in Figure 2.4, eccentricity and q_2 have a linear relationship [13]. Therefore, for a high q_2 or eccentric event, one would expect more out-of-plane suppression than in-plane, and for a low eccentric or q_2 event, in-plane and out-of-plane suppression would be almost identical.

Chapter 3

Evaluation and Discussion

This section aims to provide a thorough analysis on the following comparisons that can be made for each of the models that were used.

3.1 Glauber Analysis

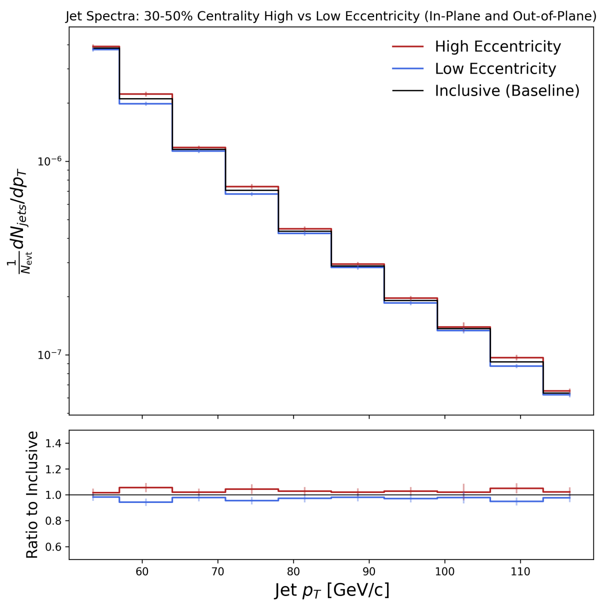

Figure 3.1: Plot of jet transverse momentum for events with high and low eccentricity for the Glauber model.

Due to the elongation of the major axis in the collision region, there are slightly more jets in high eccentric events than low eccentric events as shown in Figure 3.1, which is also the reason why the histograms and the ratios in Figure 3.3b lie below the inclusive baseline. But this difference is small, since both ratios are very close to 1.

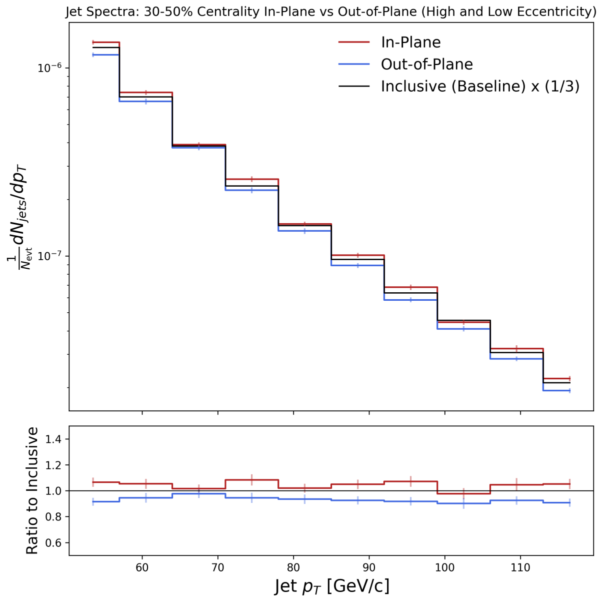

Figure 3.2: Plot of in-plane and out-of-plane jet spectra using the Glauber model, for both high and low eccentric events. The baseline is scaled by one-third to account for the selected angular region covered by in-plane and out-of-plane jets.

The reason why Figure 3.2 shows that there are more in-plane jets than those out-of-plane would be due to higher out-of-plane suppression. This is a direct consequence of path-length dependence, and can be further explained using Figure 3.3a and 3.3b. Using the eccentricity bounds found in Chapter 2, Figure 3.3a and 3.3b show path-length dependence, and it can be seen that for low eccentric events, the in-plane and out-of-plane jet spectra are nearly identical. This is to be expected as the collision region is more spherical than elliptical, thereby the number of out-of-plane jets and in-plane jets are almost identical as shown in their ratios being quite close to 1. While, for high eccentric events as given in Figure 3.3a, the reason for the larger difference lies in out-of-plane jets having to travel a much longer distance than in-plane jets, thereby leading to greater suppression.

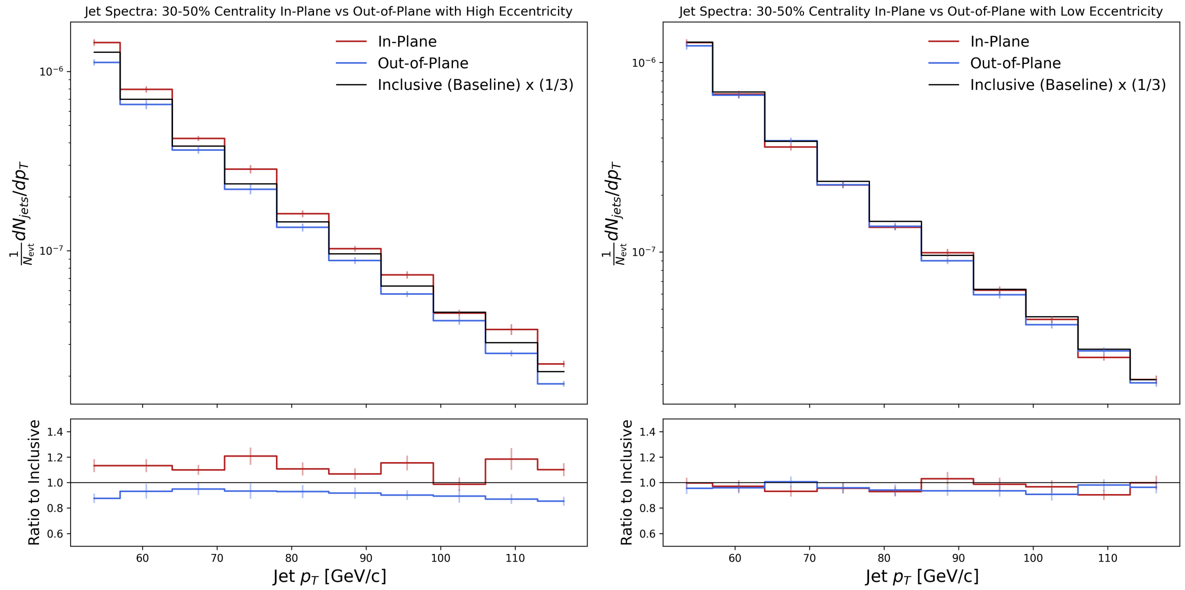

(a) Comparison with high eccentricity

(b) Comparison with low eccentricity

Figure 3.3: Comparison of in-plane and out-of-plane jets using the Glauber model, with high and low eccentricity.

3.2 Trajectum Analysis

The jet spectra for high and low eccentricity events is shown in Figure 3.4.

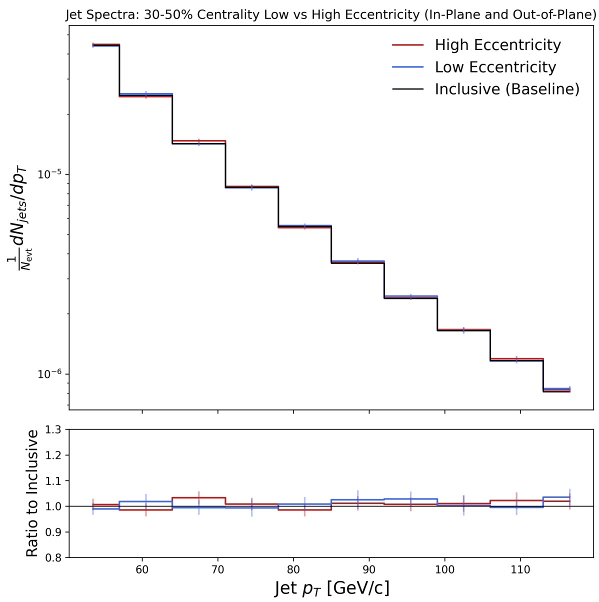

Figure 3.4: Comparison of jet p_T spectra in high and low eccentricity events, using Trajectum.

Conducting an analysis for Trajectum based on initial state eccentricity also gives a strong indication for jet suppression path-length dependence as shown in Figure 3.5. This effect can be highlighted further when considering Figures 3.6a and 3.6b.

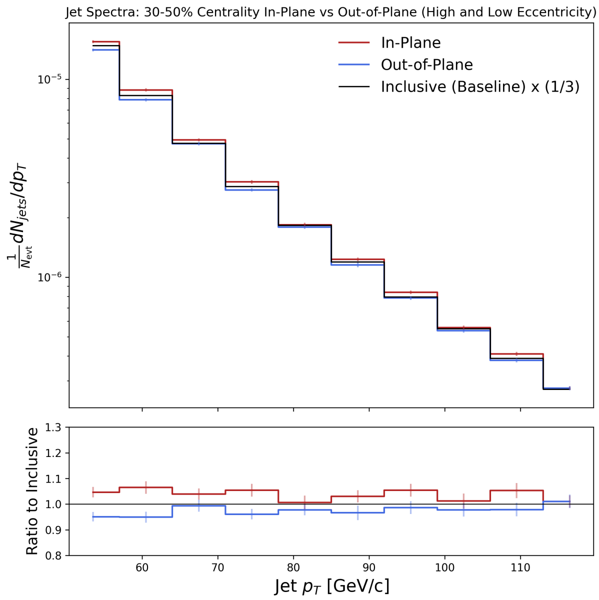

Figure 3.5: Plot of in-plane and out-of-plane jet spectra, using Trajectum for high and low eccentric events.

Now as done previously with the Glauber model, path-length dependence was tested as shown in Figures 3.6a and 3.6b. Even taking the error bars into consideration, one could still note that there exists path-length dependence in jet suppression. For high eccentric events, there are fewer out-of-plane jets compared to in-plane ones, while for low eccentric events, the difference is unclear just as for the Glauber model. This confirms that path-length dependency exists for Trajectum even in the initial state, and further proves that this effect is independent of the model chosen.

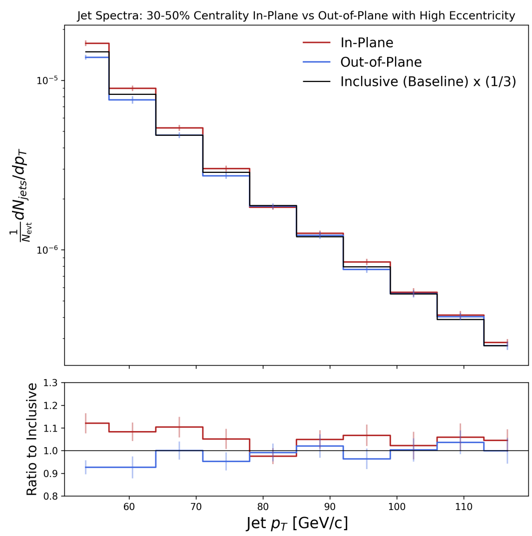

(a) Comparison with high eccentricity

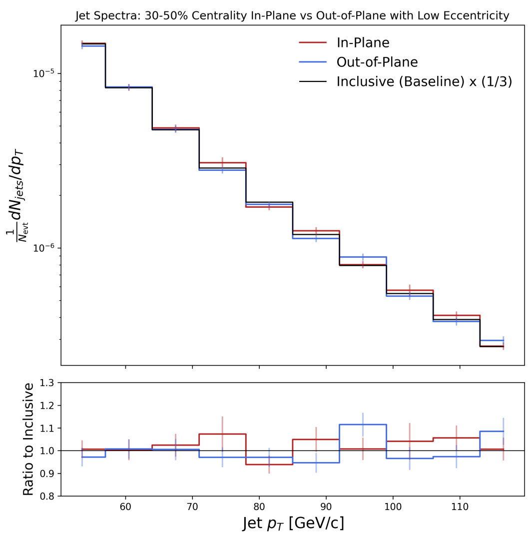

(b) Comparison with low eccentricity

Figure 3.6: Comparison of in-plane and out-of-plane jets with high and low eccentricity, using Trajectum.

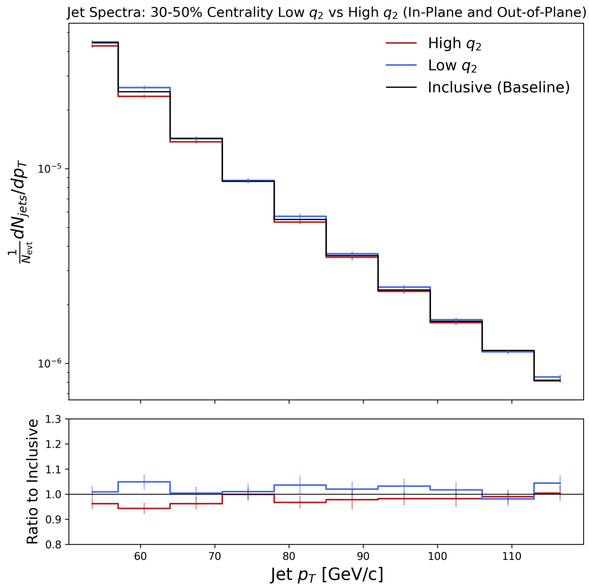

Figure 3.7: Jet transverse momentum spectra for low and high q_2 events, using Trajectum.

As seen by the ratio plot in Figure 3.7, the ratios of both high and low q_2 jets are close to 1, meaning that there are almost as many jets produced from high q_2 events as there are for low q_2. The reason for there being slightly fewer jets in high q_2 than low q_2 events could be because the simulations are conducted in a centrality class of 30 – 50%, and the low q_2 events seen possibly come from more central collisions, but further investigation is required.

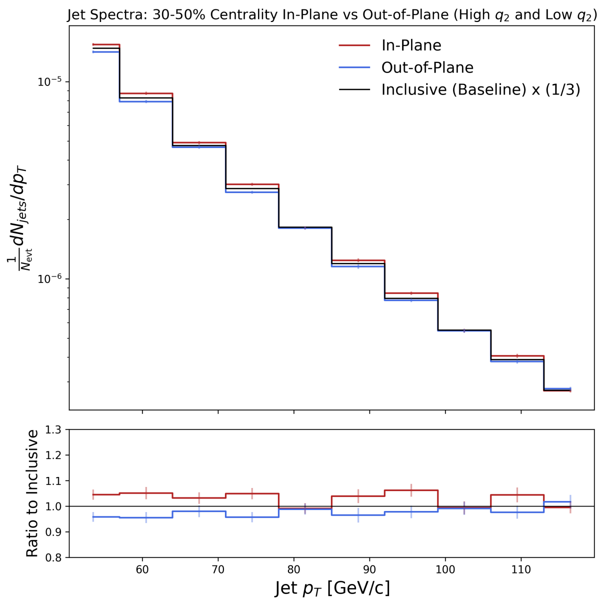

Figure 3.8: In-plane and out-of-plane jet spectra using Trajectum, for events with high and low q_2. The inclusive baseline is scaled by one-third to include the selected angular region covered by in-plane and out-of-plane jets.

Figure 3.8 is as expected showing more out-of-plane jet suppression than in-plane, and as before with eccentricity, this is a signal that indicates path-length dependence in jet quenching. To illustrate this effect further, Figures 3.9a and 3.9b directly demonstrate path-length dependence in jet suppression. High q_2 events provide a larger distance for out-of-plane jets to travel and thereby lead to more suppression than for in-plane jets. For low q_2 events the jet spectra are more identical.

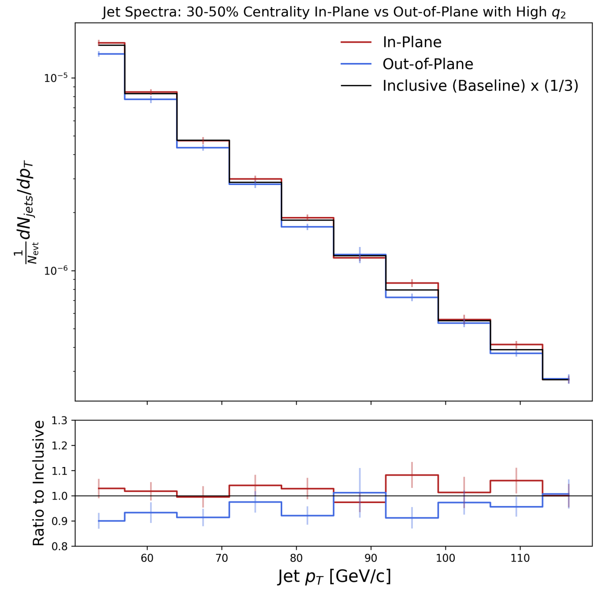

(a) Comparison with high q_2

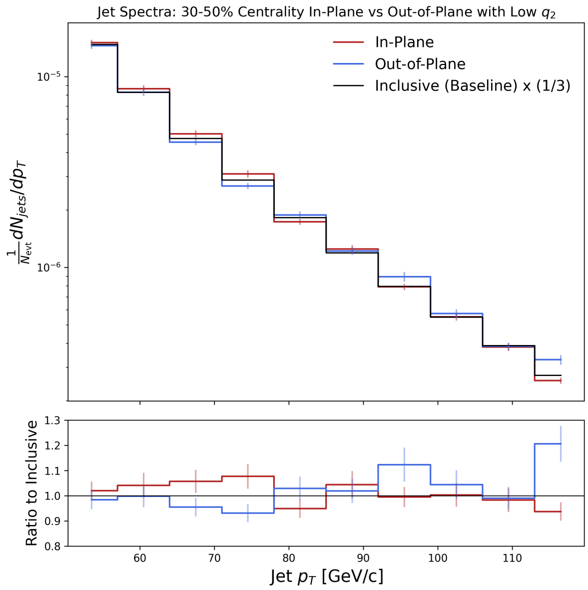

(b) Comparison with low q_2

Figure 3.9: Comparison of in-plane and out-of-plane jets using Trajectum with high and low q_2. The selected angular region covered by in-plane and out-of-plane jets is taken into consideration by scaling the baseline by one-third.

As a summary, observing Figures 3.4, 3.7, and 3.1 demonstrates the need to consider the orientation of jets, because all the aforementioned figures show almost the same number of jets, regardless of the event's eccentricity or q_2 magnitude. Figures 3.2, 3.8, and 3.5 show greater out-of-plane suppression than in-plane suppression, but these alone are not sufficient to demonstrate path-length dependence because the difference in path length is still small. This is why Figures 3.6, 3.3, and 3.9 clearly show path-length dependence in jet suppression, since we are selecting highly eccentric events. This also means that JEWEL was successful in simulating this effect and reproducing Figure 1.5.

Chapter 4
Conclusion and Outlook

This thesis aimed at examining path-length dependence for jet suppression in a medium known as QGP, using JEWEL, a Monte-Carlo event generator. JEWEL was able to successfully simulate the medium such that it was possible to qualitatively replicate the study done by the ALICE collaboration as given in Figure 1.5 and also, gave valuable insights into the physics of jet suppression. The degree of this suppression depends on how far the jet must travel through the medium. This distance depended on either eccentricity or q_2, which determined the geometric shape of the QGP. Both these factors were shown to be proportional to one another.

Eccentricity was used to classify the shape of the initial state, while q_2 is calculated from the final state and would require the momenta of the final state particles of the QGP after hydrodynamic expansion, which was not available in the Glauber model, as it was used to only simulate the initial state of the QGP. The final state was covered by Trajectum, and in both models, it was observed that jets moving out-of-plane were more suppressed than those moving in-plane. Furthermore, in order to show that this effect was independent of the model selected, plots similar to those constructed using events from the Glauber model were observed using events taken from Trajectum. Also, it is important to note that the difference between in-plane and out-of-plane jets is small if we do not choose jets based on eccentricity, which highlights the significance of considering the geometry of the QGP for analysing jet suppression.

Additionally, a by-product of the correlation between q_2 and eccentricity was indicated by the fact that the difference in suppression between out-of-plane and in-plane jets was larger for high q_2 and high eccentricity than for low q_2 and low eccentricity, which directly shows a path-length dependency. It was, however, curious to find that there were slightly fewer jets produced from high q_2 events than for low q_2. What would cause this to occur? Perhaps a more in-depth investigation is necessary. Finally, as this thesis gives a qualitative analysis, a logical next step would be to expand this to a quantitative study using experimental data.

Bibliography

[1] ALICE Collaboration. "Modification of charged-particle jets in event-shape engineered Pb–Pb collisions at $\sqrt{s_{\mathrm{NN}}} = 5.02$ TeV." In: *Physics Letters B* 851 (2024), p. 138584. DOI: 10.1016/j.physletb.2024.138584. arXiv: 2307.14097 [nucl-ex].

[2] B. Alver and G. Roland. "Collision-geometry fluctuations and triangular flow in heavy-ion collisions." In: *Phys. Rev. C* 81 (5 May 2010), p. 054905. DOI: 10.1103/PhysRevC.81.054905. URL: https://link.aps.org/doi/10.1103/PhysRevC.81.054905.

[3] Francisco Alves Barreiro. "Geometrical Aspects of Jet Quenching in Small Systems." MA thesis. Nov. 2022.

[4] Christian Bierlich et al. *A comprehensive guide to the physics and usage of PYTHIA 8.3.* 2022. arXiv: 2203.11601 [hep-ph]. URL: https://arxiv.org/abs/2203.11601.

[5] Christian Bierlich et al. "Robust Independent Validation of Experiment and Theory: Rivet version 3." In: *SciPost Physics* 8.2 (Feb. 2020). ISSN: 2542-4653. DOI: 10.21468/scipostphys.8.2.026. URL: http://dx.doi.org/10.21468/SciPostPhys.8.2.026.

[6] Megan Connors et al. "Jet measurements in heavy ion physics." In: *Reviews of Modern Physics* 90.2 (June 2018). ISSN: 1539-0756. DOI: 10.1103/revmodphys.90.025005. URL: http://dx.doi.org/10.1103/RevModPhys.90.025005.

[7] Matt Dobbs and Jørgen Beck Hansen. "The HepMC C++ Monte Carlo event record for High Energy Physics." In: *Computer Physics Communications* 134.1 (2001), pp. 41–46. ISSN: 0010-4655. DOI: https://doi.org/10.1016/S0010-4655(00)00189-2. URL: https://www.sciencedirect.com/science/article/pii/S0010465500001892.

[8] Wojciech Florkowski. *Phenomenology of Ultra-Relativistic Heavy-Ion Collisions.* WORLD SCIENTIFIC, 2010. DOI: 10.1142/7396. eprint: https://www.worldscientific.com/doi/pdf/10.1142/7396. URL: https://www.worldscientific.com/doi/abs/10.1142/7396.

[9] Qing-Fei Han, Man Xie, and Han-Zhong Zhang. "Jet cone size dependence of single inclusive jet suppression due to jet quenching in Pb+Pb collisions at $\sqrt{s_{NN}} = 5.02$ TeV." In: *Physical Review C* 113.4 (Apr. 2026). ISSN: 2469-9993. DOI: 10.1103/1j7c-rmkn. URL: http://dx.doi.org/10.1103/1j7c-rmkn.

[10] Ulrich Heinz and Björn Schenke. *Hydrodynamic Description of the Quark-Gluon Plasma.* 2024. arXiv: 2412.19393 [nucl-th]. URL: https://arxiv.org/abs/2412.19393.

[11] Marco António Coelho Leitão. "QGP effects on Energy Correlators inside jets." MA thesis. Instituto Superior Técnico, Universidade de Lisboa, Dec. 2023.

[12] Govert Nijs et al. "Bayesian analysis of heavy ion collisions with the heavy ion computational framework Trajectum." In: *Physical Review C* 103.5 (May 2021). ISSN: 2469-9993. DOI: 10.1103/physrevc.103.054909. URL: http://dx.doi.org/10.1103/PhysRevC.103.054909.

[13] Jacquelyn Noronha-Hostler et al. "Linear and cubic response to the initial eccentricity in heavy-ion collisions." In: *Phys. Rev. C* 93 (1 Jan. 2016), p. 014909. DOI: 10.1103/PhysRevC.93.014909. URL: https://link.aps.org/doi/10.1103/PhysRevC.93.014909.

[14] B. R. Webber. *Fragmentation and Hadronization*. 1999. arXiv: hep-ph/9912292 [hep-ph]. URL: https://arxiv.org/abs/hep-ph/9912292.

[15] Korinna C. Zapp. "JEWEL 2.0.0: directions for use." In: *Eur. Phys. J. C* 74.2 (2014), p. 2762. DOI: 10.1140/epjc/s10052-014-2762-1. arXiv: 1311.0048 [hep-ph].

[16] Korinna C. Zapp, Frank Krauss, and Urs A. Wiedemann. "A perturbative framework for jet quenching." In: *JHEP* 03 (2013), p. 080. DOI: 10.1007/JHEP03(2013)080. arXiv: 1212.1599 [hep-ph].

Appendices

Appendix A
Code Repository

The source code for the data processing and analysis is available at the following repository: `https://github.com/DMN564/Thesis`

Appendix B
Tables

Parameter	Purpose
LOGFILE	Provides log files for each run with JEWEL.
HEPMCFILE	Provides path to HEPMC files.
PTMIN	Provides minimum transverse momentum of jets.
PTMAX	Provides maximum transverse momentum of jets.
ETAMAX	Provides maximum rapidity.
SQRTS	Provides the center of mass energy of the collision.
WEXPO	Provides oversampling for weighted events.
NEVENT	Provides the number of collisions.
KEEPRECOILS F	Provides recoil effects.
WRITESCATCEN F	Provides output for thermal momentum subtraction.
WRITEDUMMIES F	Provides dummy particles for 4-momentum subtraction.
CENTRMIN	Provides the minimum centrality
CENTRMAX	Provides the maximum centrality

Table B.1: Table detailing parameters that will be used

Quantity	Purpose
Npart_proj	Defines number of projectile participants.
Npart_targ	Defines number of target participants.
impact_parameter	Defines b.
event_plane_angle	Defines azimuthal angle of event plane.
eccentricity	Defines eccentricity of particpants in the transverse plane.

Table B.2: Table detailing HEPMC parameters

Histogram	Purpose
`Ecc`	Eccentricity
`Q2`	q_2
`P_t_50`	Jets with a 50 GeV p_T cut
`P_t_50_Out_Plane`	Out-of-plane jets
`P_t_50_In_Plane`	In-plane jets
`P_t_50_Low_Ecc`	Jets with a 50 GeV p_T cut with low eccentricity
`P_t_50_High_Ecc`	Jets with a 50 GeV p_T cut with high eccentricity
`P_t_50_Out_Plane_Low_Ecc`	Out-of-plane jets with low eccentricity
`P_t_50_Out_Plane_High_Ecc`	Out-of-plane jets with high eccentricity
`P_t_50_In_Plane_Low_Ecc`	In-plane jets with low eccentricity
`P_t_50_In_Plane_High_Ecc`	In-plane jets with high eccentricity
`P_t_50_Low_Q2`	Jets with a 50 GeV p_T cut with low q_2
`P_t_50_High_Q2`	Jets with a 50 GeV p_T cut with high q_2
`P_t_50_Out_Plane_Low_Q2`	Out-of-plane jets with low q_2
`P_t_50_Out_Plane_High_Q2`	Out-of-plane jets with high q_2
`P_t_50_In_Plane_Low_Q2`	In-plane jets with low q_2
`P_t_50_In_Plane_High_Q2`	In-plane jets with high q_2

Table B.3: Table detailing the histograms that will be used